Available online at www.sciencedirect.com

ScienceDirect

Ceramics International 36 (2010) 55–61

CERAMICS INTERNATIONAL

www.elsevier.com/locate/ceramint

The role of MgO on the structural properties of $CaO–Na_2O(MgO)–P_2O_5–CaF_2–SiO_2$ derived glass ceramics

S.M. Salman [*], S.N. Salama, H. Darwish, E.A. Mahdy

Glass Research Department, National Research Centre, El-Behoos St., Dokki, Cairo 12622, Egypt

Received 20 April 2009; received in revised form 1 June 2009; accepted 29 June 2009
Available online 17 July 2009

Abstract

The effect of increasing MgO/Na_2O replacements (on mole basis) on the crystallization characteristics of glasses based on the $CaO–Na_2O(MgO)–P_2O_5–CaF_2–SiO_2$ system were studied by using DTA, XRD, and SEM. The crystallization characteristics of the glasses, the type of crystalline phases formed and the resulting microstructure were investigated. The main crystalline phases formed after controlled heat-treatment of the base glass were diopside, wollastonite solid solution, fluoroapatite and sodium calcium silicate phases. The increase of MgO at the expense of Na_2O led to decrease the amount of sodium calcium silicate phase. The Vicker's microhardness values (5837–3362 MPa) of the resulting glass–ceramics were markedly improved by increasing the MgO-content in the glasses. The obtained data were correlated to the nature and concentration of the crystalline phases formed and the resulting microstructure.

Keywords: Glass; Crystallization characteristics; Microhardness

1. Introduction

Glass–ceramic materials are polycrystalline solids with a residual glassy matrix leading to a characteristic microstructure that allows achievement of a better performance to abrasiveness and an increased resistance compared to traditional glasses. The microstructure of such material can be also obtained by a sintering process where crystallization and densification of glass particles occur during firing [1].

Calver et al. [2] studied the influence of fluorine content on the crystallization behaviour of $CaO–MgO–SiO_2–P_2O_5–F^-$ glassy system. They found that all glasses of composition $(50.28 - x)$ CaO–7.11 MgO–35.46 SiO_2–7.15 P_2O_5–x CaF_2, where ($x = 0$, 0.4, 4.77) were crystallized to glass ceramic containing apatite and wollastonite phases. Apatite crystallizes at lower temperature than wollastonite, the former favouring bulk nucleation and the latter exhibits surface nucleation.

Mechanism of crystallization of apatite and wollastonite phases were studied by Galliano and Poroto [3] in a glass of composition 44.7 CaO–4.6 MgO–34 SiO_2–16.2 P_2O_5 and 0.5 CaF_2 wt.%. The glass was heat-treated at 749–851 °C to form apatite phase and then at 925–1025 °C where the wollastonite phase was crystallized. They also noticed that the initial crystallization of wollastonite was very fast and also increases with temperature.

Salama et al. [4] prepared glass–ceramics from 33.32 CaO–20.1 MgO–40.76 SiO_2–4.36 P_2O_5–1.46 CaF_2 (mol%), with minor amounts of Na_2O, B_2O_3 and TiO_2. They showed that diopside and fluoroapatite crystalline phases were the main phases developed. The product has linear expansion coefficient (25–500 °C) 10.0×10^{-6}/°C and microhardness value is 7085 MPa. Tulyaganov [5] stated that there is no evidence for the formation of solid solution phases or liquid immiscibility gaps between diopside and fluoroapatite phases.

Kokubo et al. [6] succeeded to prepare a high strength glass–ceramics in the $CaO–MgO–SiO_2–P_2O_5$ system (A–W glass ceramics). They found that the crystallization of the parent glass in a bulk form led to the occurrence of large cracks. This was attributed to the precipitation of fibrous β-wollastonite after precipitation of fluoroapatite, however, crystallization of the same glass in a powder form, cracks-free glass–ceramic formed due to the crystallization of both apatite and wollastonite fine crystals throughout the glass article. Shyu and Wu [7] and Liu and Chou [8] have studied the crystallization of glass–ceramic, that

---

[*] Corresponding author. Tel.: +20 2 33370931.
E-mail address: saadmoghazy@hotmail.com (S.M. Salman).

0272-8842/$36.00. Crown Copyright © 2009 Published by Elsevier Ltd and Techna Group S.r.l. All rights reserved.
doi:10.1016/j.ceramint.2009.06.021

being based on the MgO–CaO–SiO_2–P_2O_5 system. They found that this glass–ceramic system had a superior strength and fracture toughness when compared to the apatite–wollastonite material.

Mastelaro et al. [9] studied the crystallization characteristics of the Na_2O–CaO–SiO_2 system. They detected ($Na_2Ca_2Si_3O_9$) crystalline phase after heat-treatment at crystallization temperature of 690 °C.

The aim of the present work is to study the crystallization characteristics of the glasses based on CaO–Na_2O(MgO)–P_2O_5–CaF_2–SiO_2 system. The choice of the present system is based on some interesting mineral phases that could be synthesized from the glasses of such system which reflect on the properties of the resultant materials.

2. Experimental procedure

2.1. Batch composition and glass preparation

In the present work, a systematic study of the crystallization characteristics and microhardness of some glasses based on the CaO–Na_2O(MgO)–P_2O_5–CaF_2–SiO_2 system modified by increasing the amount of MgO instead of Na_2O are considered (Table 1). The glass batches were prepared from reagent grade powders of $CaCO_3$, $MgCO_3$, Na_2CO_3, $NH_4H_2PO_4$, quartz (SiO_2) and CaF_2. The components of the batch after being accurately weighed were thoroughly mixed in agate mortar for about 15 min to ensure complete homogeneity. The weighed batches were melted in Pt–2%Rh crucibles, covered with platinum cap to minimize the evaporation, in an electric furnace with SiC heating elements at 1200–1350 °C for 3 h. The homogeneity of the melt was achieved by stirring the melt several times at about 30 min intervals, the melt was cast into rods, squares and buttons which were then properly annealed in a muffle furnace at 650 °C for 30 min to minimize the strain.

2.2. Differential thermal analysis (DTA)

The thermal behaviour of the finely powdered (45–75 μm) glass samples was examined using a SETARAM Labsys^{TM} TG-DSC16. The powdered glass was heated in Pt-holder with another one containing Al_2O_3 as a reference material. A uniform heating rate of 10 °C min^{-1} was adopted. Data were recorded using a computer-driven data acquisition system. The results obtained were used as a guide for determining the required heat-treatment temperatures applied to induce crystallization of the glasses. The progress of crystallization in the glasses was followed by double stage heat-treatment regimes. The glasses were first heated according to the DTA results at the endothermic peak temperature for 5 h, which was followed by another thermal treatment at the exothermic peak temperature for 10 h.

Table 1
The chemical compositions of the glasses (mol%).

Glass No.	Oxide contents (mol%)					
	CaO	MgO	Na_2O	P_2O_5	CaF_2	SiO_2
G_1	31.50	15.50	6.00	3.50	1.00	42.50
G_2	31.50	17.00	4.50	3.50	1.00	42.50
G_3	31.50	18.50	3.00	3.50	1.00	42.50
G_4	31.50	20.00	1.5	3.50	1.00	42.50
G_5	31.50	21.50	–	3.50	1.00	42.50

2.3. Material investigation

Identification of the crystal phases precipitating due to the course of crystallization was conducted by X-ray diffraction analysis (XRD) of the powdered samples. The X-ray diffraction patterns were obtained by using Bruker-AXS D8 Advance, with Ni filtered Cu Kα radiation. The reference data for the interpretation of the X-ray diffraction patterns were obtained from ASTM X-ray diffraction card files. The crystallization characteristics and internal microstructures of fractured surfaces of the crystalline samples, coated with gold spray, were examined by using scanning electron microscopy (SEM). Representative electron micrographs were obtained by using Jeol, JXA-840 Electron Probe Microanalyzer.

2.4. Microhardness measurements

The microhardness of the investigated samples was measured by using Vicker's microhardness indenter (SHIMADZU, HMV-2 Series, Japan). The eyepiece on the microscope of the apparatus allowed measurements with an estimated accuracy of ±0.5 μm for the indentation diagonals. The specimens were cut using a low speed diamond saw, dry ground using 1200 grit SiC paper and polished carefully using 6, 3 and 1 μm diamond paste to obtain smooth and flat parallel surfaces glass–ceramic samples before indentation. At least six indentation readings were made and measured for each sample. Testing was made using a load of 100 g; loading time was fixed for all crystalline samples (15 s). The measurements were carried out under normal atmospheric conditions. The Vicker's microhardness value was calculated from the following equation:

$$H_{\mathrm{v}}\,(\mathrm{kg/mm^2}) = A\left(\frac{p}{d^2}\right)$$

where A is a constant value equal to 1854.5 takes into account the geometry of squared based diamond indenter with an angle 136° between the opposing faces, p is the applied load (g), and d is the average diagonal length (μm). The microhardness values are converted from kg/mm^2 to MPa by multiplying with a constant value 9.8.

3. Results

3.1. Differential thermal analysis (DTA)

The DTA data (Fig. 1) of the glasses G_1–G_5 showed endothermic effects at the 700–744 °C temperature range. This effect represents the glass transition temperature (T_g), at which

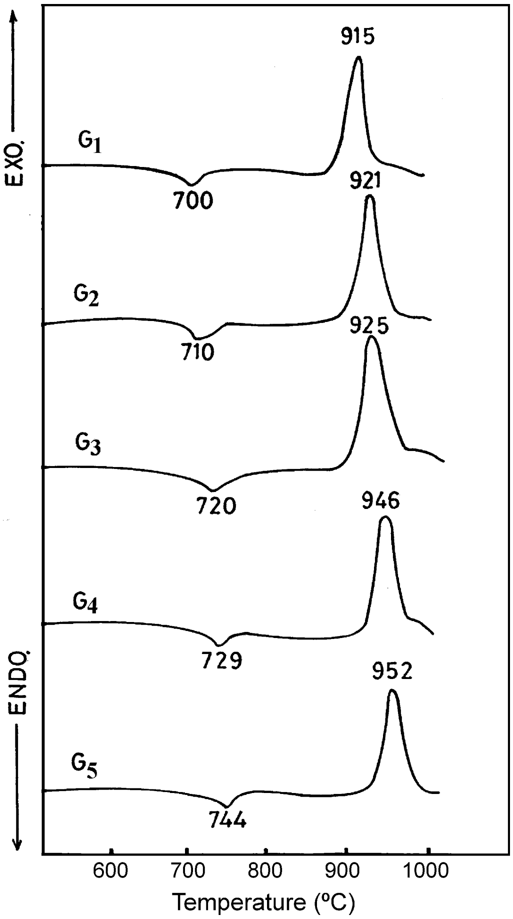

Fig. 1. DTA data of the studied glasses.

the nucleation begins. Exothermic effects at the 915–952 °C temperature range indicating that the crystallization reaction in the glass was also recorded. The DTA data (Fig. 1) revealed that the increasing of MgO at the expense of Na_2O led to shift both the endothermic dips and the onset of the crystallization exotherms to higher temperatures.

SEM micrographs of the fractured surfaces, Figs. 2–4, showed the effect of increasing MgO at the expense of Na_2O on the microstructure of the glass–ceramic samples (G_1, G_3 and G_5). The SEM micrograph (Fig. 2) of the fractured surface of the crystallized glass G_1 shows botryoidal microstructure by crystallization at 700 °C/5 h–915 °C/10 h. Fig. 3 of sample G_3 shows volume crystallization of fine fibrous and rounded-like growths which were developed by the crystallization at 720 °C/5 h–925 °C/10 h. While volume crystallization of oriented fine fibrous-like growths was formed in the crystalline sample G_5 (free of Na_2O) crystallized at 745 °C/5 h–950 °C/10 h, Fig. 4.

3.2. XRD analysis

The X-ray diffraction analysis (Fig. 5, Pattern I) revealed that the base glass G_1 thermally heated at 700 °C/5 h–915 °C/10 h, crystallized into pyroxene phase of diopsidic-type ($CaMgSi_2O_6$) (major lines 3.66, 3.22, 2.98, 2.94, 2.88, 2.56, 2.50, Card No. 19-239), together with wollastonite-like phase (wollastonite ss) (major lines 3.32, 3.22, 2.98, 2.88, 2.56, 2.50,

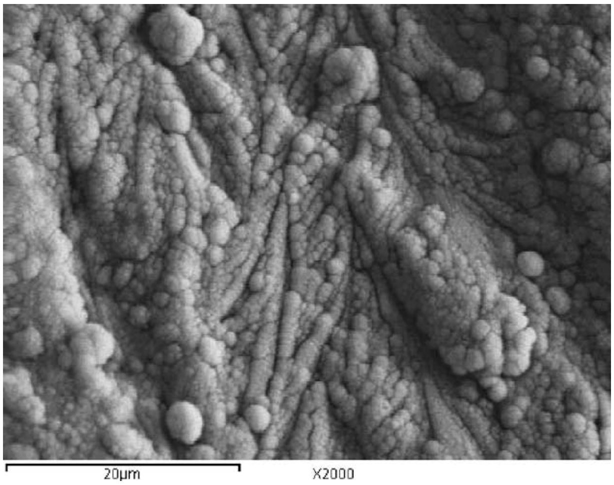

Fig. 2. SEM micrograph of fractured surface of glass (G_1), crystallized at 700 °C/5 h–915 °C/10 h, shown volume crystallization of botryoidal microstructure (2000×).

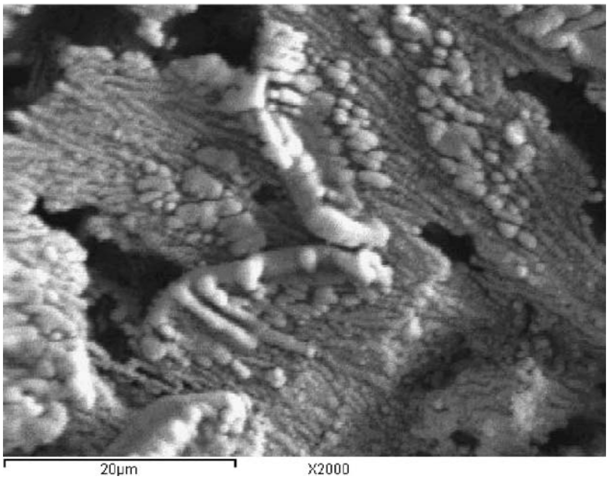

Fig. 3. SEM micrograph of fractured surface of glass (G_3), crystallized at 720 °C/5 h–925 °C/10 h, shown fine fibrous and rounded-like growths (2000×).

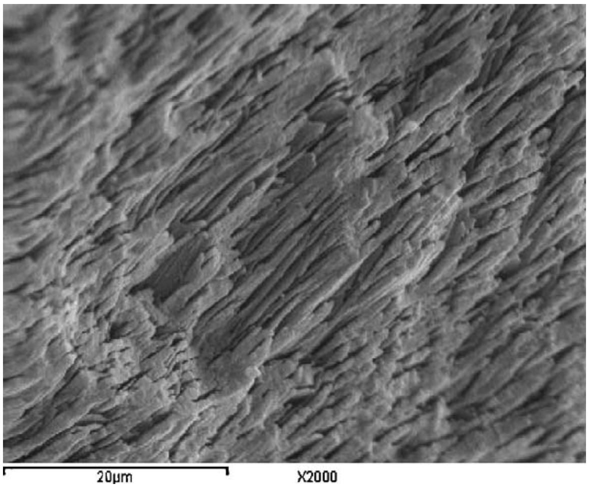

Fig. 4. SEM micrograph of fractured surface of base glass (G_5) crystallized at 745 °C/5 h–950 °C/10 h, shown volume crystallization of oriented fine fibrous microstructure (2000×).

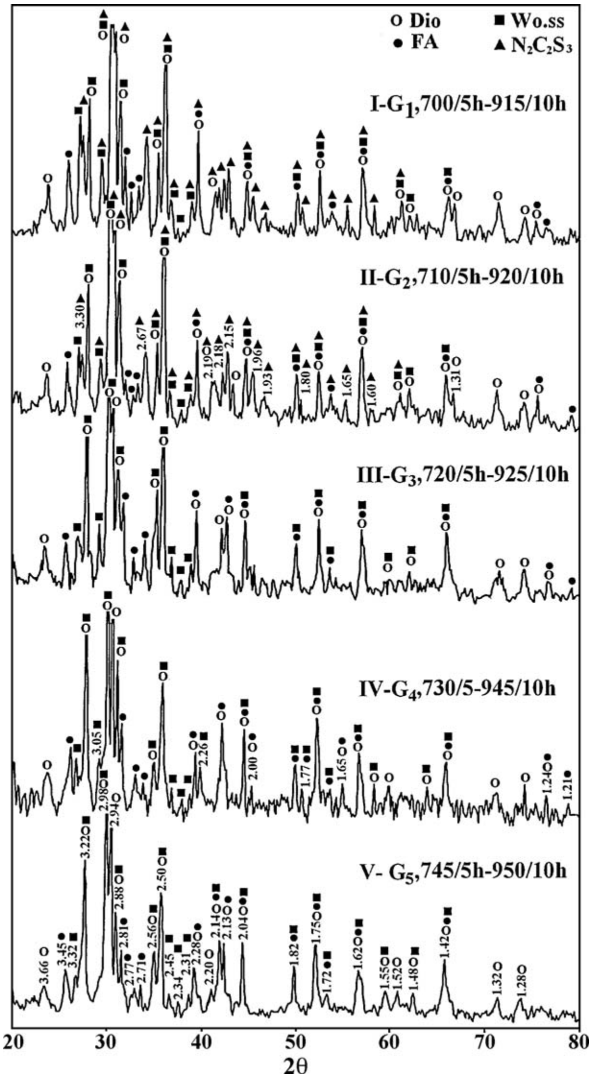

Fig. 5. XRD patterns of the studied glass–ceramics (i.e. G_1–G_5).

2.45, 2.34, 2.31, 2.14, 1.82, Card No. 29-372), fluoroapatite phase (lines 3.45, 2.81, 2.77, 2.71, 2.13, 1.82, 1.75, 1.72, Card No. 15-876) and sodium calcium silicate ($Na_2Ca_2Si_3O_9$) phase (major lines 3.30, 3.05, 2.67, 2.19, 2.18, 2.15, 1.80, 1.65, 1.60, Card No. 22-1455).

The addition of MgO at the expense of Na_2O, i.e. G_2 heat-treated at 710 °C/5 h–920 °C/10 h, led to the formation of diopside, wollastonite ss, fluoroapatite and minor amount of sodium calcium silicate phases (Fig. 5, Pattern II).

On increasing MgO addition instead of Na_2O, i.e. G_3, G_4 and G_5 heat-treated at 720 °C/5 h–925 °C/10 h, 730 °C/5 h–945 °C/10 h and 745 °C/5 h–950 °C/10 h, respectively, the X-ray diffraction analysis of the crystallization products revealed that diopside, wollastonite ss and fluoroapatite phases were crystallized and no Na-containing phases could be detected (Fig. 5, Patterns III, IV and V, Table 2).

3.3. Microhardness

Vicker's microhardness property was determined for resulting glass–ceramics. The microhardness values of the investigated glass–ceramic materials were exhibited in Table 2. The data are also graphically represented in Fig. 6 from which the following outlines could be concluded.

The increase of MgO at the expense of Na_2O in the base glass (G_1) generally led to increase the microhardness values of the crystalline samples (e.g. G_2–G_5). The value of sample G_5 (free of Na_2O) exhibits the highest hardness value, while the sample G_1 (with high Na_2O content) represents the lowest value (Table 2 and Fig. 6).

4. Discussion

4.1. Crystallization characteristics

4.1.1. The crystallization characteristics of the base glass

The crystallization process of the glass during the reheating process is known to be connected with the nature and proportions of the glass oxide constituents. The ability of some cations to build glass forming units or to be housed as modifiers in interstitial positions in the glass structure should also be considered [10].

The addition of MgO at the expense of Na_2O in the studied glasses increased the temperature at which crystallization started, The DTA data clearly indicated that both the temperatures of the nucleation endotherm and crystallization exotherm were increased by adding MgO instead of Na_2O. Sodium oxide was a good glass modifier and has beneficial effect in lowering the temperature of the glass to convert it into glass–ceramic. It could be housed in the glass structure in the interstices positions which increase the number of groups between the (SiO_4) chains, i.e. decrease the SiO_4 chain [11,12]. MgO of stronger single bond strength than that of Na_2O [13], can share in the glass structure as MgO_4 group forming tetrahedral coordination due to the presence of the large amount of oxygens available from the Na_2O present in the glass compositions. This may account for the increase of the coherency of the glass structure which resulted into a compact structure [11]. The MgO/Na_2O replacement causes the glass

Table 2
The crystalline phases developed and microhardness values of the investigated glass–ceramics (i.e. G_1–G_5).

Glass No.	Heat-treatment (°C/h)	Microhardness (MPa)	Developed phases
G_1	700/5 h–915/10 h	3362	Diopside + Wollastonite ss + Fluoroapatite + Sodium calcium silicate
G_2	710/5 h–920/10 h	3951	Diopside + Wollastonite ss + Fluoroapatite + Sodium calcium silicate (minor)
G_3	720/5 h–925/10 h	4396	Diopside + Wollastonite ss + Fluoroapatite
G_4	730/5 h–945/10 h	4713	Diopside + Wollastonite ss + Fluoroapatite
G_5	745/5 h–950/10 h	5837	Diopside + Wollastonite ss + Fluoroapatite

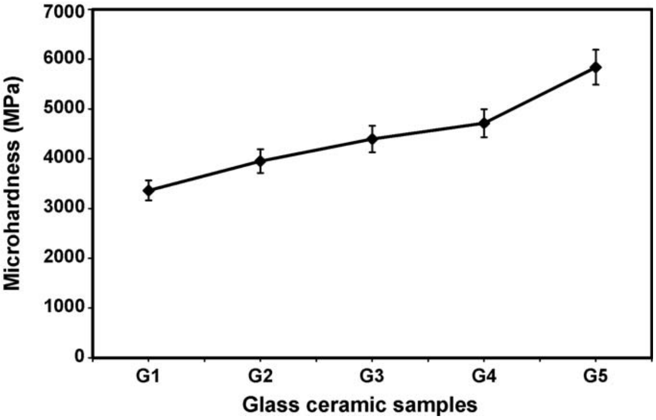

Fig. 6. Microhardness values of the studied glass–ceramics (i.e. G_1–G_5).

structure to stiffen, increase the viscosity of the glass which hinders the diffusion of the different ions. Therefore, the tendency of the glass–crystalline conversion becomes more difficult by addition of MgO instead of Na_2O.

The sequence of the phases development during crystallization of the base glass (G_1) revealed that diopside ($CaMgSi_2O_6$) was formed as a major phase together with wollastonite solid solution, fluoroapatite and sodium calcium silicate phases.

Theoretically, on the basis of the petrochemical calculation of normative mineral molecules [14] it was found that diopside-$CaMgSi_2O_6$, could be formed as a major constituent, while wollastonite ($CaSiO_3$), fluoroapatite ($Ca_5(PO_4)_3F$) and sodium calcium silicate ($Na_2Ca_2Si_3O_9$) phases were crystallized as secondary phases from crystallization of the base glass G_1. Thus, during crystallization of the glass, CaO could combine with equivalent amount of MgO together with the proper amount of SiO_2 to form diopside according to the following schematic equation:

$$CaO + MgO + 2SiO_2 \rightarrow CaMgSi_2O_6$$

Some of the CaO present in the glass could combine with the corresponding amount of the remaining silica to form wollastonite as follows:

$$CaO + SiO_2 \rightarrow CaSiO_3$$

However, the present results revealed that wollastonite solid solution phase was developed instead of wollastonite phase as indicated from the shift of d-spacing lines (XRD) characteristics for wollastonite phase towards higher 2θ values.

Pyroxenes consist of a group of minerals of variable composition, which crystallized fairly readily. They are closely related in crystallographic and other physical properties, as well as, in chemical composition [12]. A wide variety of ionic substitution occurs in the members of the pyroxene group and there is a solid solution between the group components, e.g. diopside ($CaMgSi_2O_6$) and wollastonite ($CaSiO_3$).

It seems, therefore, that wollastonite can accommodate diopside molecule in its structure to form wollastonite ss. Deer et al. [12] reported that, wollastonite can take up to 22% of diopside ($CaMgSi_2O_6$) phase in its structure. It assumed therefore that the preferential formation of wollastonite solid solution phase was favoured by the great affinity of the wollastonite to accommodate the diopside component in solid solution.

It is well known that compositions crystallizing to give solid solution series are important to control the properties of the resultant materials, and offer an excellent opportunity to the glass–ceramic study [15].

Toya et al. [16] have reported that diopside is a preferable crystalline phase since it results in stronger materials than glass–ceramics based on wollastonite.

It should be noted that more Ca^{2+} ions are included in the phosphate-rich phases because P^{5+} ions has a higher ionic field strength and hence a greater tendency to shielding. It was also reported by Taniguchi et al. [17] that P_2O_5 had a high tendency to react with CaO in the presence of CaF_2. Thus, fluoroapatite-$Ca_5(PO_4)_3F$ crystallized from the droplet phase with highly concentrated Ca and P [18]. Apatite is the major crystalline phase of bioactive glass ceramic that crystallizes evenly throughout the material. Synthetic fluoroapatite has been used extensively as bone implant materials due to their identical chemical composition and high biocompatibility with natural bone [19].

4.1.2. *The effect of substitution of Na_2O by MgO*

The increase of MgO-content at the expense of Na_2O in the base glass led to shift both of the endo- and exotherms of the glasses towards higher temperatures. This may be explained by the increasing effect of MgO on the rigidity of these glasses [5] by forming MgO_4 tetrahedra with the SiO_4 group.

The addition of MgO, in replacing Na_2O, led to the formation of diopside, wollastonite ss, fluoroapatite and sodium calcium silicate phases. $Na_2Ca_2Si_3O_9$ is a non-stoichiometric phase [20]. It seemed therefore that the remaining of CaO present in the glass could combine with a corresponding amount of the Na_2O and the remaining amount of SiO_2 to form sodium calcium silicate as follows:

$$Na_2O + 2CaO + 3SiO_2 \rightarrow Na_2Ca_2Si_3O_9$$

Chen et al. [21] succeeded in the synthesized highly bioactive machineable glass–ceramic for bone engineering. They found that the mechanically strong crystalline phase $Na_2Ca_2Si_3O_9$ can transform into an amorphous calcium phosphate phase after immersion in simulated body fluid (SBF) for 28 days.

The formation of sodium-containing phases could not be detected among the crystallization products of glass of low Na_2O-containing glasses. It was suggested, therefore, that Na_2O could be present in the glassy matrix of the resultant glass–ceramic [22] and this is in a good agreement with the present X-ray results which indicate that by increasing the MgO/Na_2O replacements, diopside, wollastonite ss and fluoroapatite phases were crystallized from glasses G_3–G_5 and no $Na_2Ca_2Si_3O_9$ phase could be detected.

4.2. Microhardness

Hardness is not a fundamental physical property of material but it rather depends on several properties. Its interpretation varies considerably depending on the nature of the material under examination and the method of test under consideration. Therefore, the resistance of the material to abrasion under closely specified conditions may be taken as one measure of hardness [23].

Henry and Hill [24] reported that the microstructure mostly represents the major influence on the mechanical properties of the glass ceramic materials. They found that hardness of fluorosilicate glass–ceramics decreased markedly due to the development of the coarse microstructure in the glass–ceramics. The mechanical properties of glass–ceramics, among other variables, depend on volume fraction, grain size, crystal phase and shape of crystals [25].

The addition of MgO at the expense of Na_2O in the base glass (G_1) increased the microhardness values of the investigated glass–ceramics (G_2–G_5). This may be due the formation of fine fibrous microstructure as indicated from the SEM micrograph of the glass–ceramics of G_3 and G_5 (Figs. 3 and 4), as compared with that of botryoidal microstructure formed in the glass–ceramic of G_1 (Fig. 2).

The high microhardness value (5837 MPa) measured for the crystalline glass, G_5, may be due to the formation of oriented fine fibrous microstructure as indicated from SEM (Fig. 4) and also to the crystallization of high microhardness diopside phase (major), together with wollastonite ss and fluoroapatite phases. Park et al. [26] indicated that glass–ceramics containing large amount of diopside phase generally showed a high microhardness value due to the interlocking microstructures of diopside crystals with microhardness value 6730 MPa. Sohn et al. [27] revealed that the hardness of silicate glass–ceramics increased due to the fine grained microstructure by which the crystal size plays an important role in preventing the propagation of the cracks in the whole structure. The microhardness of glass–ceramics generally increased with the increase of the crystallizability, smaller crystalline grains as well as formation of fine microstructure [28].

Lin et al. [29] reported that in general, the porosity and grain size are key factors affecting on the strength of glass–ceramics, the strength of ceramic material increased with the decrease in the porosity and grain size.

5. Conclusions

The crystallization characteristics and microhardness of the glass–ceramics based on the $CaO–Na_2O(MgO)–P_2O_5–CaF_2–SiO_2$ system, modified by increasing MgO-content at the expense of Na_2O were investigated. The addition of MgO in replacing Na_2O in the glass had an effect on the type of the crystalline phases formed and microstructures of the resulting glass–ceramic. Diopside (major), wollastonite ss and fluoroapatite phases could be obtained together in some cases with sodium calcium silicate phase. The types of the crystallized phases formed and their microstructures were discussed in relation to the compositional variation of the parent glasses. The microhardness values (5837–3362 MPa) of the investigated glass–ceramics were markedly improved by the addition of MgO at the expense of Na_2O.

References

[1] M.G. Rasteiro, G. Tiago, R. Santos, E. Antunes, Crystalline phase characterization of glass–ceramic glazes, Ceram. Int. 33 (2007) 345–354.

[2] A. Calver, R.G. Hill, A. Stamboulis, Influence of fluorine content on the crystallization behaviour of apatite wollastonite glass–ceramics, J. Mater. Sci. 39 (2) (2004) 2601–2603.

[3] P. Galliano, L.J. Poroto, Kinetics of crystallization of apatite and wollastonite from a bioactive glass of the calcia–silica magnesia–phosphorous pentaoxide–calcium fluoride system, in: 35th Annual Congr. Bras. Ceram. III Iberoam. Ceram., Vidrios Refract., Part 2, 1991, 758–765.

[4] S.N. Salama, H. Darwish, H.A. Abo-Mosallam, HA forming ability of some glass–ceramics of the $CaMgSi_2O_6–Ca_5(PO_4)_3F–CaAl_2SiO_6$ system, Ceram. Int. 32 (2006) 357–364.

[5] D.U. Tulyaganov, Phase separation and devitrification in the fluoroapatite diopside system, in: XIX Proceeding of the International Congress on Glass, vol. 2, Edinburgh, Scotland, July 1–6, 2001, p. 198 (Extended Abstract).

[6] T. Kokubo, S. Ito, S. Sakka, T. Yamamura, Formation of a high strength bioactive glass–ceramic in the system magnesium oxide–calcium oxide–silica–phosphorous pentaoxide, J. Mater. Sci. 21 (2) (1986) 536–540.

[7] J.J. Shyu, J.M. Wu, Effects of composition changes on the crystallisation behaviour of $MgO–CaO–SiO_2–P_2O_5$ glass–ceramics, J. Am. Ceram. Soc. 74 (9) (1991) 2123–2130.

[8] D.M. Liu, M.M. Chou, Formation of a new bioactive glass ceramic, J. Mater. Sci.: Mater. Med. 5 (1994) 7–10.

[9] V.R. Mastelaro, E.D. Zanotto, N. Lequeux, R. Cortes, Relationship between short rang order and ease of nucleation in $Na_2Ca_2Si_3O_9$, $CaSiO_3$ and $PbSiO_3$ glasses, J. Non-Cryst. Solids 262 (2000) 191–199.

[10] Y.J. Park, P.J. Bary, Determination of the structure of glasses in the manganese borate ($MnO–B_2O_3$) system using ^{11}B NMR, J. Korean Phys. Soc. 14 (1) (1981) 67–74.

[11] H. Scholze, Glass: Nature, Structure and Properties, Springer-Verlag, NY, 1990.

[12] W.A. Deer, R.A. Howie, J. Zussman, An Introduction to the Rock-forming Minerals, Third ELBS Impression, Common Wealth, Printing Press Ltd., Hong Kong, 1992.

[13] J. Zarzycki, Glass and Vitreous State, Cambridge University Press, NY, Port Chester, 1991.

[14] T.F. Barth, Theoretical Petrology, 2nd ed., Wiley, NY, 1962.

[15] S.N. Salama, Glass ceramics containing some varieties of Mn-solid solution phases, Mater. Chem. Phys. 28 (1991) 237.

[16] T. Toya, Y. Kameshima, A. Yasumori, K. Okada, Preparation and properties of glass–ceramic clay wastes (kira) of silica and kaolin clay refining, J. Eur. Ceram. Soc. 24 (2004) 2367–2372.

[17] T. Taniguchi, M. Okuno, T. Matsumoto, J. Non-Cryst. Solids 21 (1997) 56.

[18] Y. Liu, Q. Xiang, Y. Tan, X. Sheng, Nucleation and growth of needle-like fluoroapatite crystals in bioactive glass–ceramics, J. Non-Cryst. Solids 354 (2008) 938–944.

[19] I. Sevim, M. Kulekci, Abrasive wear behavior of bioactive glass–ceramics containing apatite, Bull. Mater. Sci. 29 (2006) 243–249.

[20] G.K. Moir, F.P. Glasser, Phase equilibria in the system $Na_2SiO_3–CaSiO_3$, Phys. Chem. Glasses 15 (1) (1974) 6–11.

[21] Q.Z. Chen, I.D. Thompson, A.R. Boccaccini, 45S5 Bioglass®-derived glass–ceramic scaffolds for bone tissue engineering, Biomaterials 27 (2006) 2414–2425.

[22] S. Agathopoulos, D.U. Tulyaganov, J.M.G. Ventura, S. Kannan, A. Saranti, M.A. Karakassides, J.M.F. Ferreira, Structural analysis and devitrification of glasses based on the $CaO–MgO–SiO_2$ system with B_2O_3, Na_2O, CaF_2 and P_2O_5 additives, J. Non-Cryst. Solids 352 (2006) 322.

[23] P.W. McMillan, Glass–Ceramics, Academic Press, London, NY, 1979.

[24] J. Henry, R.G. Hill, The influence of lithia content on the properties of fluorphlogopite glass–ceramics. II. Microstructure hardness and machineability, J. Non-Cryst. Solids 319 (2003) 13–30.

[25] W. Höland, G.H. Beall, Glass–Ceramic Technology, Am. Ceram. Soc., Inc., 2002.

[26] Y.J. Park, S.O. Moon, J. Heo, Crystalline phase control of glass–ceramics obtained from sewage sludge fly ash, Ceram. Int. 29 (2003) 223–227.

[27] S.B. Sohn, S.Y. Choi, Y.K. Lee, Controlled crystallization and characterization of cordierite glass–ceramics for magnetic memory disk substrate, J. Mater. Sci. 35 (2000) 4815–4821.

[28] F.J. Torres, J. Alarcon, Mechanism of crystallization of pyroxene based glass–ceramic glazes, J. Non-Cryst. Solids 347 (2004) 45–51.

[29] K. Lin, W. Zhai, S. Ni, J. Chang, Y. Zeng, W. Qian, Study of the mechanical property and *in vitro* biocompatibility of $CaSiO_3$ ceramics, Ceram. Int. 29 (2) (2004) 223–227.